

Energy & Environmental Science

Accepted Manuscript



This is an *Accepted Manuscript*, which has been through the Royal Society of Chemistry peer review process and has been accepted for publication.

Accepted Manuscripts are published online shortly after acceptance, before technical editing, formatting and proof reading. Using this free service, authors can make their results available to the community, in citable form, before we publish the edited article. We will replace this *Accepted Manuscript* with the edited and formatted *Advance Article* as soon as it is available.

You can find more information about *Accepted Manuscripts* in the [Information for Authors](#).

Please note that technical editing may introduce minor changes to the text and/or graphics, which may alter content. The journal's standard [Terms & Conditions](#) and the [Ethical guidelines](#) still apply. In no event shall the Royal Society of Chemistry be held responsible for any errors or omissions in this *Accepted Manuscript* or any consequences arising from the use of any information it contains.

Optimization of the neutralization of Red Mud by pyrolysis bio-oil using a Design of Experiments Approach.

Véronique Jollet, Christopher Gissane and Marcel Schlaf*

Abstract

A factorial design and response surface approach has been employed to optimize the neutralization, partial reduction, magnetization and carbonization of highly alkaline Red Mud bauxite residue as derived from the Bayer process using highly acidic pyrolysis bio-oil as the limiting reagent. Explored was the impact of the factors temperature, reaction time and – most importantly – the minimum bio-oil/Red Mud ratio required. The significant response parameters evaluated were: the minimization of the sodium content and the quantity of the aqueous phase, the maximization the carbon content and magnetization of the solid neutralized Red Mud phase as well as the stabilization of the *pH* of both phases close to 7. The optimum process parameters determined provide a starting point for a possible scale-up and suggests a potential pathway for the environmental remediation of Red Mud lagoons using a renewable biomass derived resource.

Keywords: pyrolysis; bio-oil; Red Mud; factorial design; process design

Table of Contents Graphics



Co-processing alkaline Red Mud (bauxite residue) with acidic pyrolysis bio-oil yields a gray pH-neutral solid containing ~ 30 % (w/w) biomass derived carbon and magnetic iron suboxides.

Broader Context

Strong yet lightweight aluminium metal is a critical component of our civil and transportation infrastructure – and it has dirty secret: for every ton of pure Al_2O_3 , which is electro-refined into aluminium metal, the processing of aluminium bauxite ore produces 1-2 tons of a highly alkaline residue (pH 10-13) commonly referred to as Red Mud. ~ 120 million tons of this material are generated per year and to date ~ 3,000 million tons have been stored as a slurry in open air lagoons surrounded by dams all over the world with no final economically and ecologically viable remediation or recycling solution in sight. As recent tragic events in Kolontár, Hungary harshly demonstrated (10 fatalities and a 647 million US\$ fine for environmental damages) structural failure of the dams of these storage sites can have catastrophic consequences requiring a costly long-term stewardship of the lagoons. Recognizing that the most problematic and hazardous aspect of Red Mud is its alkalinity, we propose that acidic bio-oils produced by the pyrolysis (i.e., rapid heating with exclusion of air) of agricultural and forestry by-products could be used as a renewable biomass derived resource to neutralize and therefore remediate the Red Mud to a harmless or even value-added material.

Introduction

Annually more than ~ 120 million tons of Red Mud bauxite residue generated by the Bayer process for the production of alumina are stored in lagoon or dry-stacking sites worldwide with an estimated 3 gigatons of material having been accumulated to date.¹⁻⁴ The high alkalinity (typically $pH \geq 12$) of this material is an issue due its toxicity towards all plant and animal life and at present no large scale solution is available to permanently remediate this waste storage problem.⁵

As previously demonstrated by others and ourselves, Red Mud can be used as a catalyst for various processes,⁶⁻¹⁶ including the upgrading of an acidic pyrolysis bio-oil generated by the fast pyrolysis of hardwood chips or other agricultural and forestry by-products.¹⁷⁻²² In a complementary approach, we here propose that the normally problematic high acidity of the bio-oil can be exploited by using it as a biomass derived renewable low-cost limiting reagent for the neutralization and hence remediation of Red Mud^{23,24-26} Figure 1 gives a flow-chart of the overall process envisioned.

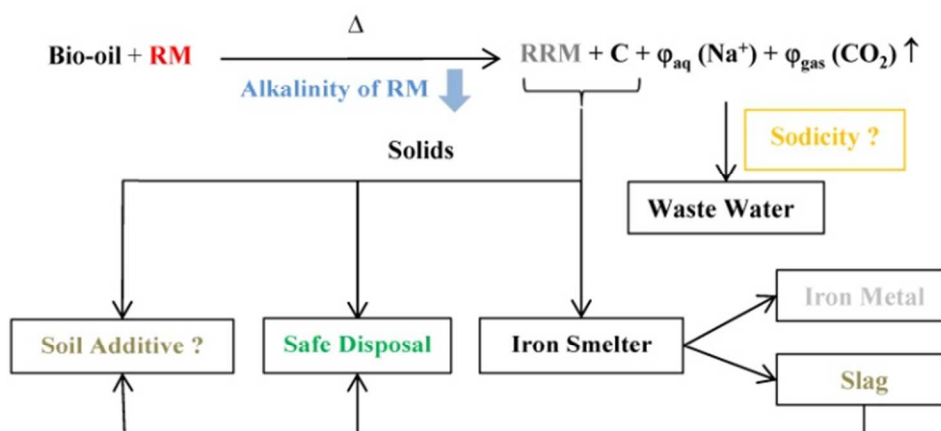


Figure 1: Process for the neutralization of Red Mud with pyrolysis bio-oil.

The reaction between Red Mud and bio-oil at elevated temperature and autogenic pressure in a sealed reactor results in the formation of a *pH*-neutral magnetized solid product phase, rendering the product non-hazardous and potentially valuable as an iron ore or iron binder containing significant amounts of biomass derived carbon. Depending on the actual and ultimate composition – notably sodium and possible heavy metal content – of the solid product obtained it or any slag resulting from processing as an iron ore could possibly also be used as a soil additive or component of building materials.²⁷⁻²⁹

In order to show how to study and design the co-processing of Red Mud with bio-oil, a factorial design of experiments (DOE) approach was used to plan and conduct experiments aimed at optimizing the process parameters.³⁰⁻³² The specific objective of the study was to determine the minimum amount of pyrolysis bio-oil required for an effective neutralization of Red Mud and establish the viable experimental conditions and the influence of process variables on the overall process. To this end, the effects of *temperature*, *reaction contact time* and *bio-oil/Red Mud ratio* were evaluated using a full factorial matrix with the monitored output parameters being the *pH of the solid product* (as an aqueous extract), the *amount of carbon deposited* into the solid product and its *magnetic susceptibility* χ (an indirect measure of the amount of reduced iron sub-oxides Fe_xO_y present).^{33, 34} The partial reduction and the deposition of carbon into the reduced material with the bio-oil serving as the source of both the carbon and the reductant requires the rejection of oxygen as either carbon dioxide or water and leads – by chemical necessity – to the formation of an aqueous phase as the by-product of the reaction.²¹ Therefore the *pH of the liquid by-product phase* (ϕ_{aq}), its *mass* and *sodium content* (sodicity) were also tracked, as a large amount of sodium leaching from the Red Mud into this aqueous product phase or a $\text{pH} > 8$ or < 6 of this phase will prevent or at least complicate its safe disposal impacting the economic and ecologic

viability of the proposed process. Furthermore, a central composite matrix was used to explore the response surfaces and determine the optimal values for the combination of all process parameters for an acceptable compromise.^{35, 36}

Results and Discussion

Table 1 gives the reaction parameters for temperature, contact time and Bio-Oil/Red Mud ratio. The ranges chosen are based on the values established empirically in our earlier studies, which showed that the activation of Red Mud as a catalyst occurs at ~ 330 °C,¹⁹ and that a minimum mass ratio bio-oil/Red Mud of 3:1 is necessary to generate an organic liquid product phase at a 4 h contact time at temperature.²¹ Aiming to explore the effect of lowering both these parameters to – for the purpose of Red Mud neutralization – more favourable values, mass ratios were fixed at 2:1 and 1:1 and contact times at 2.25 and 0.5 h. The maximum temperature was set to 365 °C, in order to avoid potentially reaching the supercritical point ($T > 373$ °C) of the water generated in the reaction mixture, which could introduce a hard to interpret discontinuity into the DOE approach and also result in unpredictable process pressure changes. Using the same, but significantly aged bio-oil as in our previous study that aimed at the use of Red Mud as an upgrading catalyst, the reactions conducted at all of the bio-oil/Red Mud mass ratios employed did not generate any liquid organic product phase, i.e., all organic material was either fully adsorbed in to the solid dark gray product phase or decomposed into CO₂ (identified by micro-GC in gas phase samples from the headspace of the reactor). This is consistent with our earlier observation that the aged bio-oil resists upgrading to liquid product phases.²¹ The aqueous liquid product phase generated did not contain significant amounts of organics (by GC/GC-MS).

Full Factorial Experimental Design

The initial experimental implementation was conducted using a full factorial matrix. Tables 2 and 3 list the codification and levels of the independent variables considered and the design matrices for all experiments conducted (see Experimental Section for further details). The responses and results of this study are collected in Table 4. The coefficients of the fitted model were calculated and used to quantify the effect of the factors on the studied responses. The different factors have more or less impact according to the importance of the coefficient values. The ranking of the variation identified by each source is visible on the Pareto graphs given in the Supplementary Information. In the second Pareto graph, the less important variables were removed out of the full model. The validity of the hypothesis for the residuals of the linear regression was verified using graphical tests also shown in the Supplementary Information. By increasing the degrees of freedom when the number of terms to be determined is reduced, the forms of the residuals plots are improved. The coefficients of the fitted model obtained after refining the less important terms are presented in Table 5.

Based on the contribution of individual terms to R^2 of the model (β values), the greatest contribution found is that of the temperature (X_1) on the mass magnetic susceptibility. This is not surprising as heating promotes the formation of reduced iron species in particular magnetite (Fe_3O_4), which has a substantially higher magnetic susceptibility than the initial species Fe_2O_3 , hematite and $\text{FeO}(\text{OH})$, goethite present in the Red Mud. The weight of the contribution of each factor revealed that the bio-oil/Red Mud ratio (X_3) had the most significant effect on the $p\text{H}$, the sodium content and the mass of the aqueous phase and the $p\text{H}$ of and the amount of carbon deposited into the gray magnetized solid product phase. The important effect of the bio-oil/Red Mud ratio on the mass of the aqueous phase generated and the percentage of carbon deposited

into the solid product phase indicates that almost all of the water and carbon originates from the pyrolysis bio-oil (crude oil composition weight percentages: ~ 37 % of water by Karl Fischer titration and ~ 35 % of carbon by Elemental Analysis) with only a negligible contribution from the Red Mud (~ 1% of water; < 0.6% of carbon). The impact importance of the bio-oil/red ratio on the *pH* of the two phases also revealed that the final *pH* obtained is principally related to the initial amount of the acidic bio-oil and its capacity to neutralize the alkalinity of the Red Mud.

A variance test was carried out using a Student t-test to assess the significance of each variable in the model. *p*-values lower than 0.05 indicate that a given model variable is considered significant and contributes significantly towards the response. The statistical coefficients at the 95% confidence level are highlighted in bold in Table 5. According to the *p*-value, the order of significance of the independent variables on the desired neutral target *pH* of the solid phase is X_3 followed by X_1 . Furthermore, all the variables (X_1 , X_2 , X_3) and the interaction between the reaction time and the bio-oil/red ratio X_2X_3 have a significant impact on the mass of the aqueous phase. The significant influence of the factors temperature and reaction time on these responses can be explained by the types of the deoxygenation reactions that occur during the heating under autogenic pressure. They lead to the degradation of acids present in the bio-oil by ketonization and the formation of water and CO_2 , which also affect the *pH* of the mixture and the amount of water generated.¹⁹⁻²¹ Furthermore, the interaction between the temperature and the reaction time (X_1X_2) is significant for the sodium content of the aqueous product phase, which means that in this case these parameters must be considered together, as the variation of the factor X_1 and X_2 individually are not significant (*p*-value of β_1 and $\beta_2 > 0.05$). This is also visible in the factorial plots in the Supplementary Information, where the mean effects plot of the sodium content shows an almost constant slope for X_1 and X_2 , whereas the interaction plot shows a high slope

for X_2 when X_1 is fixed. Based on the interaction plot, the sodium content is minimized at the edges and the center of the domain, i.e., the coordinates $(X_1; X_2)$ equal to (305; 4), (335; 2.25) and (365; 0.5).

Finally, the levels of significant coefficients were fixed at the optimal desired conditions for each significant factor and are summarized in Table 6. It appears that the bio-oil/red-mud ratio and the temperature are the most significant factors. Moreover, the best process condition to minimize the formation of an aqueous phase is a relatively short contact and reaction time of 30 minutes, i.e., the least energy consuming scenario. Consequently, the reaction time was fixed at lower level, i.e., 30 min. for the response surface study discussed below.

However, a linear regression is typically too simple to reliably fit the response and to consider the use of model for predictions. The quality of our model was therefore also evaluated by analyzing the curvature term. This term corresponds to the difference between the real value of the response at the middle of the domain obtained from the center points and the coefficient β_0 given by the regression equation. According to the p-values, the pH of the aqueous phase ($p = 0.006$) and the percentage of carbon in the solid ($p = 0.017$) have a significant curvature. We therefore further refined the model by correcting the curvature employing a matrix with quadratic terms.

Central Composite Design

Table 3 gives the composite design matrix. The responses and results of the central composite design study with the reaction time held constant at 30 min. are collected in Table 7. Some values of responses (runs 1,2,5 and 6) from Table 4 were re-used in Table 7. The final models obtained for prediction were converted to the uncoded variables in Table 8, denoted by equations

4 to 9. Those equations were used to plot the response surface graph and to simulate the responses. Despite the lower correlation coefficients achieved between 82 - 99% and 69 - 98% for R^2 and the R_{adj}^2 respectively, the fitted model reasonably describes the experimental results and trends.

Figure 2 shows the surface plot of each of the studied responses at different temperatures and bio-oil/Red Mud ratios. The surface plot of mass magnetic susceptibility clearly shows that the temperature has the strongest effect. The most important effect on the other responses is the bio-oil/Red Mud ratio. These results confirm those obtained from the full factorial matrix approach.

A variance test for the complete composite design was carried out as summarized in Table 9. The statistical coefficients at the 95% confidence level are highlighted in bold. The quadratic term X_2^2 significantly affects the magnetic susceptibility, the amount of carbon deposited and the pH of the solid and the aqueous phase, which indicates that the second order equation is suitable for fitting the process parameters for the neutralization of Red Mud by bio-oil. From the data a ratio of 2:1 bio-oil/Red Mud gives an optimum, i.e., the highest value for the mass magnetic susceptibility. Furthermore, the response surfaces for the pH of both product phases do not indicate a unique target point or region towards a desirable neutral pH as function of the process parameters.

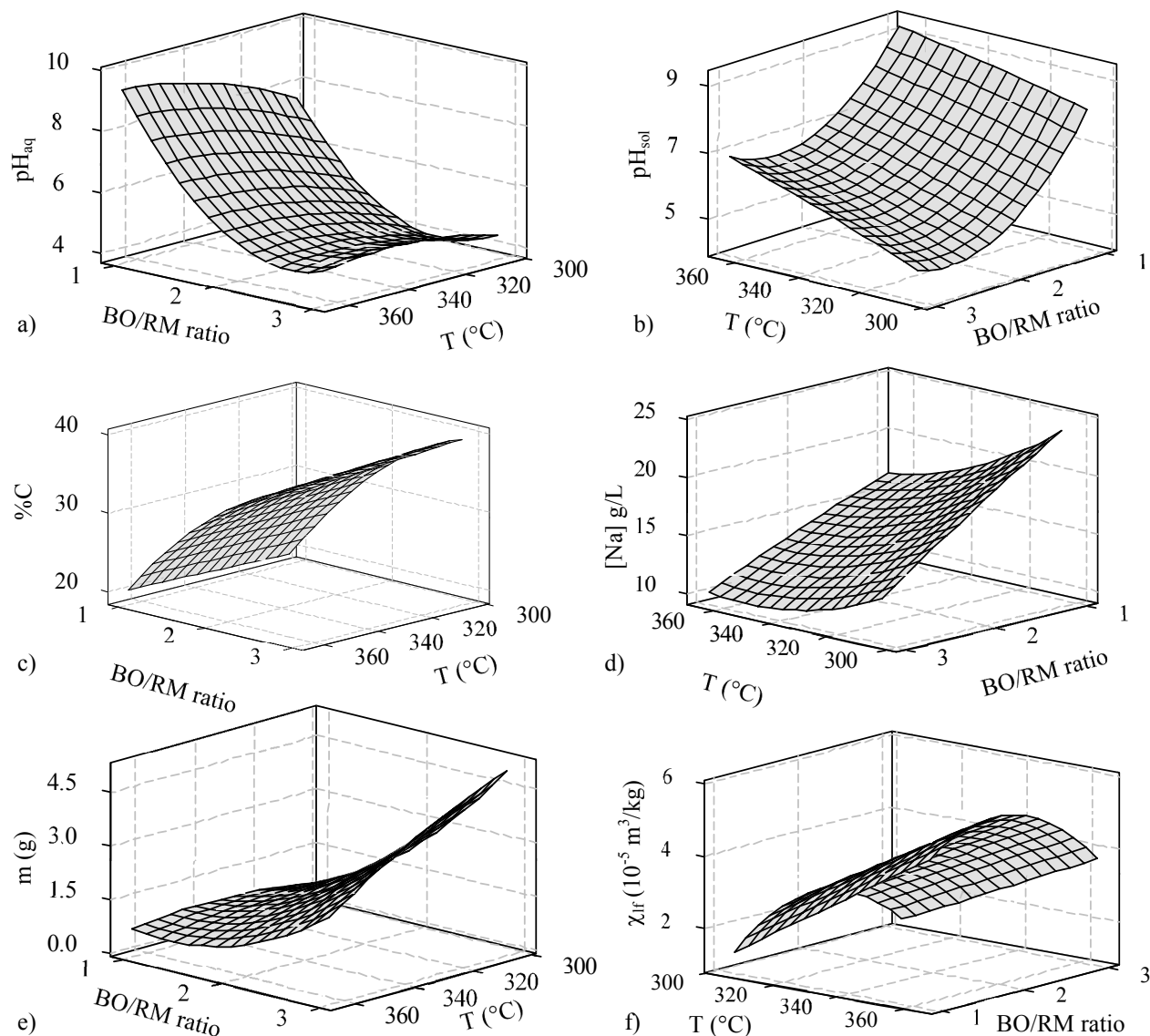


Figure 2: Response surface plotting the effects of temperature and bio-oil/Red Mud ratio over: (a) pH of the aqueous phase (b) pH of the solid (c) percentage of carbon (d) sodium content (e) mass of aqueous phase (f) mass magnetic susceptibility. Surfaces are given by equation (4-9) Table 8.

The ANOVA for the regression revealed that the model is statistically significant for all the studied responses (p -values < 0.05). Moreover, the computed F values are higher than the tabulated F -value at a significance level of 0.05 which is $F_{0.05,5,7} = 3.97$ (with $F_{\alpha,DF(m),DF(r)}$ where $DF(m)$ is the degree of freedom for the model equal to $p-1$ and $DF(r)$ the degree of freedom for

the residual error equal to $n-p$), where the number of coefficients to be determined is $p = 6$ and the number of run $n = 13$. Those results affirm that the as-fitted multiple regression model of coded variables adequately represent the observed data.

A lack of fit (LOF) test was also carried out in order to determine whether the model was adequate to describe the observed data, or whether a more sophisticated model should be used instead. Since the obtained p -values for the LOF were 0.054, 0.318 and 0.556 for the pH , the amount of carbon deposited and the mass magnetic susceptibility of the solid respectively, i.e., larger than 5%, there is statistically insignificant LOF test at 95% confidence interval. However, the LOF is not statistically significant at 99.9, 99.7 and 97.4% confidence level for the pH of the aqueous phase, aqueous mass and sodium content, respectively. In those cases, a new model could be needed.

The surface of each studied responses predicted by the model are combined in an overall contour plot depicted in Figure 3 to find the optimized operating conditions for a potential future process.

The criteria for an optimized process are

- Minimization of the sodium content and the quantity of the aqueous phase.
- Maximization of the carbon content and magnetization of the solid phase
- Stabilization of the pH of both phases as close to 7 as possible.

The area where the range for each response is satisfactory is shown in white. The middle point of the white area is obtained at a bio-oil/red-mud ratio of 1.53 and a temperature of 349 °C. Based on these chosen inputs, the area of compromise is quite limited as a lot of different responses are considered.

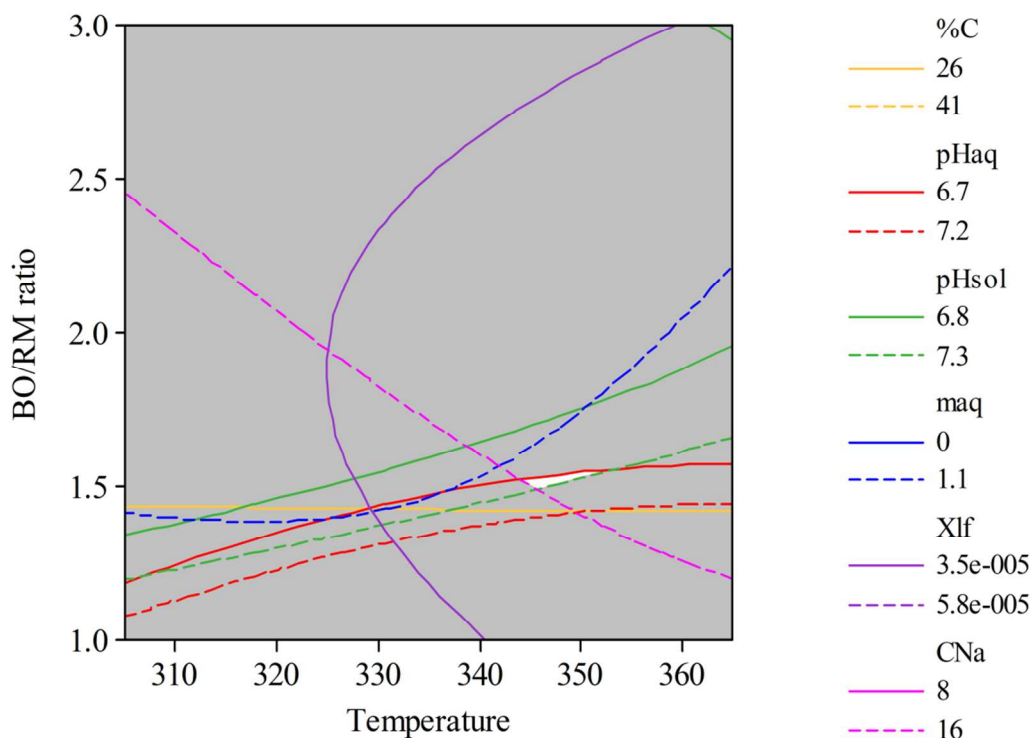


Figure 3: Contour plot of the pH of the aqueous phase, pH of the solid, mass of aqueous phase, percentage of carbon, mass magnetic susceptibility and sodium content.

Four replicates at these optimized conditions were carried out to test the experimental reproducibility and assess the validation of the regression model. The individual responses are compiled in Table 10 (runs 14 to 17), together with the calculated average, the standard deviation, the predicted response given by equation 4 to 9 and their variation range. The boundaries of the prediction interval are evaluated using the equation (10), where $y(x_0)$ is the estimate of the mean response predicted by the model, σ is the standard deviation of the model, x_0 the column vector of the level of the independent variables at a particular point, x'_0 the transpose vector of x_0 and $t_{\alpha, n-p}$ the t-value at a significance level of α (0.05).

$$y_0 = y(x_0) \pm t_{\alpha, n-p} \sqrt{\sigma^2 (1 + x'_0 (X'X)^{-1} x_0)} \quad (10)$$

This gives a 95 % confidence level that, for a single experiment, the actual response will be inside the prediction intervals. As Table 10 shows, the experimental values obtained for all the response are in fact located in the variation range confirming the acceptable predictive capability of the regression equations 4-9 (Table 8). The standard deviations are within 1 - 15 % of the average for all the responses indicating that the reaction to reaction reproducibility is acceptable considering that a very complex composition of materials is involved in the experiments and that the overall scale of the experiments is small resulting in comparatively large errors in material transfer to and from the reactor. This also explains the large deviations for the mass of the recovered aqueous phase (48 %). Even small amounts of water retained inside the channels of the reactor head used or within the solid can result in the comparatively wide variation observed inasmuch as the aqueous mass gathered at the end is very low (0 - 2.35 g) in relation to the total product mass (13 g).

A scale up by factor 2 and 3 (the maximum amounts attainable with the benchtop equipment available) was implemented to provide an initial assessment of the principle portability of the neutralization process parameters from the lab bench scale to a larger and ultimately pilot or production plant scale. The response values (runs 18 and 19 in Table 10) are similar and also located in the variation range of the prediction except for the mass of the aqueous phase. These results suggest that a good control of the properties of the products is still effective after increasing the reagent quantities and that the process as analyzed and optimized may in fact be scalable.

Magnetic Separation

The solid phases from the experiments 14 to 19 were subjected to wet magnetic separation tests, in order to establish whether a concentration of the iron content of the material could be realized in this way. The results were very similar for each sample. Less than 1% of the samples remained as the final non-magnetic product, which means that almost the totality of the particles in the solid product phase have magnetic properties. Thus, the desired magnetite or other magnetic iron suboxide or carbide species are not separable from the other oxide (aluminum, titanium, calcium, sodium oxides and silica) present in the matrix of the solid with this technique, which is likely due to a homogeneous particle dispersion of the magnetic materials throughout the reduced Red Mud, which in turn reflects the very small average particle size of the starting Red Mud (70 % < 10 μm).

Experimental

Source of Materials: The Red Mud was supplied as a slurry by Rio Tinto Alcan's Jonquière, Quebec operations and dried to a solid of constant weight at 110 °C. The general composition of the Red Mud is given in the analysis sheet supplied in the Supplementary Information as are the results of a trace metal analysis by ICP-MS that indicated the presence of only negligible amounts of other heavy metals.

The bio-oil used is representative of a low-grade high acidity oil (~ 40 % H₂O w/w, pH = 2.8), were supplied by Abri-Tech Inc. of Namur, Quebec, Canada and is the same as those used in our previously reported upgrading study that gives details of its production and composition.²¹

Co-Processing Reactions: The reactions were carried out in a 300 mL Parr reactor (316 Stainless Steel) connected to a pressure transducer module and a thermocouple. 10 g of Red Mud

and between 10 g to 30 g of bio-oil were combined in the reactor at room temperature. The mixture was stirred with a glass-coated stir bar and heated using an electric band and a hot plate and the temperature autogenic pressure evolution (3.5 to 7.9 MPa observed depending on the conditions) monitored in real time. After the indicated time, the reactor was cooled to ambient temperature. The aqueous phase was collected using a pipette, weighed and stored in a fridge. The solid residue was dried under vacuum for 8 hours, weighed, manually ground to a uniform powder in a mortar and pestle and stored in a desiccator.

Characterization of Materials: The solid phases obtained after reactions were characterized by CHN Elemental Analysis using a Thermo Scientific Flash 2000 Elemental Analyzer. The magnetic susceptibility χ was determined using a Bartington MS2 meter equipped with MS2B Dual Frequency sensor, taking measurements at 0.46 kHz (at low frequency) and is denoted as χ_{lf} in the text. Approximately 10 g of solid was placed in polyethylene vials; exact weights and volumes were recorded to determinate density and convert the volume susceptibility value into the mass specific susceptibility. The sodium contents were analyzed by Inductively Coupled Plasma (ICP) by the University of Guelph Laboratory Services. The pH was measured using glass electrodes Metrohm. To estimate the pH of the Red Mud residue, 0.5 g of solid was placed in 5 mL of water then agitated for several minutes. A clear solution for pH measurement was obtained by centrifugation. Magnetic separations were performed by Eriez Inc, Erie, Pennsylvania with the details of the results given in the Supplementary Information.

Experimental Factorial Design: A 2^3 full factorial design matrix was defined using the values and the coded levels given in Tables 1 and 2. All other variables were kept constant, i.e., the amount of Red Mud, starting ambient atmosphere pressure and stirring rate in the reactor employed. It should be noted that the heating rate and the heating duration varied substantially

(respectively 4 - 6 °C/min and 50 - 80 min) depending on the amount of material in the reactor, the final temperature and the external temperature (22 ± 2 °C). The Minitab 16 Statistical Software package was used to generate the matrices to calculate the coefficients of the fitted model, to perform the statistical data analysis and to create charts for interpretation. The limits of experimental domain for the reaction temperature, the reaction time and the bio-oil/Red Mud ratio were defined based on our previously empirically established values used in the upgrading of the bio-oil using Red Mud as the catalyst, which employed the slightly higher mass ratio bio-oil/Red Mud = 3.5/1.²¹

For statistical calculations, the real values of the independent variables were coded as dimensionless values (X_i). Three replicates at the centre point were added (runs 9-11) to determine the experimental error and the data reproducibility. Moreover, these additional data points allow estimating potential curvatures. Then, the response surface was determined using the values and the coded levels of Tables 1 and 3, with the reaction contact time dropped as an independent variable for the central composite matrix of Table 3 (see Results section).

For 3 factors, the full factorial model is shown in Eq. I, and for 2 factors, the central composite model is shown in the Eq. II where Y is the predictive response, X_i are the input variables and β_i are constant. The term β_0 is the intercept term, β_i are the linear terms, β_{ii} are the squared terms, and β_{ij} , β_{ijk} are the interactions terms.

$$(I) Y = \beta_0 + \beta_1 X_1 + \beta_2 X_2 + \beta_3 X_3 + \beta_{12} X_1 X_2 + \beta_{13} X_1 X_3 + \beta_{23} X_2 X_3 + \beta_{123} X_1 X_2 X_3$$

$$(II) Y = \beta_0 + \beta_1 X_1 + \beta_2 X_2 + \beta_{11} X_1^2 + \beta_{22} X_2^2 + \beta_{12} X_1 X_2$$

The determination of the coefficients β in the mathematical empirical model was performed by regression analysis. The coefficients were obtained solving the matrix system of Eq. III, with X being the matrix of the level of the independent variables, X' the transpose matrix of X , y the vector of the observations, β the vector of the regression coefficients and ϵ the vector of random errors.

$$(III) y = X.\beta + \epsilon, \beta = (X'X)^{-1}X'y$$

The adequacy of the model was tested by analysis of variance (ANOVA) at a 5 % level of significance using Fisher F-test and the Student t-test. The coefficient of determination (R^2) and the adjusted coefficient (R_{adj}^2) were evaluated for the linear and quadratic model.

The R^2 value indicates how much variation in the response is explained by the fitted model.

However, the R_{adj}^2 is more relevant because it accounts for the number of factors in our model.

The R^2 and the R_{adj}^2 values found are more than 98 % and more than 93 %, respectively, for the full model. After the reduction of the number of terms, the prediction equation is simplified; therefore, the values of R^2 and the R_{adj}^2 decrease. For the reduced equation, the R^2 and the R_{adj}^2 values found are respectively between 85 - 99 % and 71 - 98 % which means the correlation between the observed values and the predicted values still satisfy a meaningful and relevant evaluation of the contribution of each influential factor.

Conclusion

The neutralization of Red Mud by a typical acidic and low-grade pyrolysis bio-oil was performed at different temperatures (305 - 365 °C), reaction times (0.5 - 4 h) and bio-oil/Red Mud ratios (1 - 3), in order to establish starting point parameters for a further pilot-scale study that eventually

may lead to an industrial scale process. A full factorial design allowed a ranking of the factors and the interactions weights that influence the reaction outcome. The most important variable in is the bio-oil/Red Mud ratio, while the economically important reaction time does not have a significant impact on most of responses and consequently was fixed at the low level (30 minutes contact/reaction time). A statistical model was used to elaborate the response surface of each response using a central composite design. Based on the range of factors included in this study, the optimized conditions to minimize the wastes (quantity of aqueous phase by-product) and their toxicity (sodium content, neutral pH), and to generate potentially value-added solid products (by maximizing the magnetization of the solid phase and stabilization of its carbon content at neutral pH) are obtained at 349 °C and with a bio-oil/Red Mud ratio of 1.53. The ANOVA and the reproducibility set revealed that the second order equation model fitting the data was good enough for prediction. Within the limits of the laboratory equipment used in the current study, the results also suggest that the process will be scalable.³⁷

While the authors realize that the process will be sensitive to the actual bio-oil and Red Mud used, we hope that the system studied and data presented will form the basis for and encourage an actual commercial exploitation of the neutralization of Red Mud waste by pyrolysis bio-oil, which may be applicable to large-scale operations, if other economic and logistical factors (i.e., regional availability of biomass, transportation cost, regulatory environment, etc.) are favourable. In a best case scenario, this may allow a synergistic co-processing of two wastes streams: Red Mud from the Aluminium industry and locally supplied pyrolysis bio-oil generated from lignocellulosic biomass, i.e., the by-products of existing agri- and silvicultural operations. This would effect the remediation of Red Mud storage sites and potentially even add value to the Red Mud waste by exploring the use of the neutralized material obtained as an iron ore, iron binder,

cement component or soil additive,³⁸ while at the same time creating an immediate market for pyrolysis bio-oil without the need for an upgrading that is typically required to render it usable as a fuel.

Acknowledgements

The authors the NSERC funded BiofuelNet Canada, Rio Tinto ALCAN and ABRI-Tech Inc. for generous financial and in-kind support.

Notes and References

^a Department of Chemistry, Guelph-Waterloo Centre for Graduate Work in Chemistry (GWC)² University of Guelph, Guelph, Ontario, N1G2W1, Canada.
mschlaf@uoguelph.ca

Electronic Supplementary Information (ESI) available: Pareto charts and residual plots of the statistical data analysis. General composition of Red Mud and results of the trace metal analysis of Red Mud by ICP-MS. Details of magnetic separation experiments (11 pages).

1. G. Power, M. Grafe and C. Klauber, *Hydrometallurgy*, 2011, **108**, 33-45.
2. C. Klauber, M. Grafe and G. Power, *Hydrometallurgy*, 2011, **108**, 11-32.
3. M. Grafe, G. Power and C. Klauber, *Hydrometallurgy*, 2011, **108**, 60-79.
4. M. Grafe and C. Klauber, *Hydrometallurgy*, 2011, **108**, 46-59.
5. V. Mymrin, H. de Araujo Ponte, O. Ferreira Lopes and A. Vazquez Vaamonde, *Green Chemistry*, 2003, **5**, 357-360.
6. S. Ordonez, H. Sastre and F. V. Diez, in *Catalyst Deactivation*, eds. B. Delmon and G. F. Froment, 1999, vol. 126, pp. 443-446.
7. S. Ordonez, H. Sastre and F. V. Diez, *J. Hazard. Mater.*, 2001, **81**, 103-114.
8. S. Ordonez, H. Sastre and F. V. Diez, *Appl. Catal., B*, 2001, **29**, 263-273.
9. S. Ordonez, H. Sastre and F. V. Diez, *Appl. Catal., B*, 2001, **34**, 213-226.
10. J. R. Paredes, S. Ordonez, A. Vega and F. V. Diez, *Applied Catalysis B-Environmental*, 2004, **47**, 37-45.
11. S. Ordonez, *Appl. Catal., B*, 2008, **84**, 732-733.
12. S. Sushil and V. S. Batra, *Appl. Catal., B*, 2008, **81**, 64-77.
13. S. B. Wang, H. M. Ang and M. O. Tade, *Chemosphere*, 2008, **72**, 1621-1635.
14. M. Balakrishnan, V. S. Batra, J. S. J. Hargreaves, A. Monaghan, I. D. Pulford, J. L. Rico and S. Sushil, *Green Chemistry*, 2009, **11**, 42-47.
15. S. Sushil and V. Batra, *The Journal of Solid Waste Technology and Management*, 2011, **37**, 188-196.
16. M. Balakrishnan, V. S. Batra, J. S. J. Hargreaves and I. D. Pulford, *Green Chemistry*, 2011, **13**, 16-24.
17. B. Klopries, W. Hodek and F. Bandermann, *Fuel*, 1990, **69**, 448-455.
18. E. Karimi, C. Briens, F. Berruti, S. Moloodi, T. Tzanetakis, M. J. Thomson and M. Schlaf, *Energy & Fuels*, 2010, **24**, 6586-6600.

19. E. Karimi, A. Gomez, S. W. Kycia and M. Schlaf, *Energy & Fuels*, 2010, **24**, 2747-2757.
20. E. Karimi, I. F. Teixeira, L. P. Ribeiro, A. Gomez, R. M. Lago, G. Penner, S. W. Kycia and M. Schlaf, *Catal. Today*, 2012, **190**, 73-88.
21. E. Karimi, A. Gomez, I. F. Teixeira, E. d. Resende, C. Gissane, Véronique Jollet, I. Aigner, F. Berruti, C. Briens, B. Hoff, N. Schrier, R. M. Lago, S. W. Kycia, R. Heck and M. Schlaf, *Appl. Catal., B*, 2014, **145**, 187-196.
22. E. C. D. Resende, C. Gissane, R. Nicol, R. J. Heck, M. C. Guerreiro, J. V. Coelho, L. C. A. d. Oliveira, P. Palmisano, F. Berruti, C. Briens and M. Schlaf, *Green Chemistry*, 2013, **15**, 496-510.
23. The high acidity of the oil is caused by the the presence of formic, acetic and other carboxylic acids (10-20 % w/w) originating from the (hemi-) cellulose component as well as free phenols and catechols originating from the lignin component of the biomass used to produce the oil.
24. D. A. Laird, R. C. Brown, J. E. Amonette and J. Lehmann, *Biofuels Bioproducts & Biorefining-Biofpr*, 2009, **3**, 547-562.
25. C. A. Mullen and A. A. Boateng, *Energy & Fuels*, 2008, **22**, 2104-2109.
26. D. Mohan, C. U. Pittman and P. H. Steele, *Energy & Fuels*, 2006, **20**, 848-889.
27. A. Xenidis, A. D. Harokopou, E. Mylona and G. Brofas, *JOM*, 2005, **57**, 42-46.
28. S. Kumar, R. Kumar and A. Bandopadhyay, *Resources Conservation and Recycling*, 2006, **48**, 301-314.
29. Y. Pontikes and G. N. Angelopoulos, *Resources Conservation and Recycling*, 2013, **73**, 53-63.
30. D. C. Montgomery, *Design and Analysis of Experiments*, John Wiley & Sons, Inc., New York, Toronto, 2009.
31. R. A. Fischer, *The Design of Experiments*, Macmillan, New York, 1935.
32. S. Soravia and A. Orth, in *Ullmann's Encyclopedia of Industrial Chemistry*, Wiley-VCH Verlag GmbH & Co. KGaA, 2000.
33. S. L. Fegade, B. M. Tande, H. Cho, W. S. Seames, I. Sakodinskaya, D. S. Muggli and E. I. Kozliak, *Chem. Eng. Commun.*, 2013, **200**, 1039-1056.
34. F. Elfighi and N. A. Amin, *Reac. Kinet. Mech. Cat.*, 2013, **108**, 371-390.
35. R. H. Myers, *Response Surface Methodology*, Allyn and Bacon Inc., Boston, 1971.
36. M. Demirel and B. Kayan, *International Journal of Industrial Chemistry* 2012, **3**, 24.
37. The authors recognize that another important parameter that was not addressed in this bench-top study, but that will be become highly relevant for a scale-up of the proposed process is the efficient mixing of the two liquid/solid feeds and- by extension - the type and configuration of the reactor used.
38. In order to establish a principle eco-system tolerance to the use of the neutralized Red Mud as a soil additive, field trials with sodium tolerant plants are planned for the near future.

Table 1: Codification and levels of 3 independent variables considered for the DOE to investigate the neutralization of Red Mud with pyrolysis bio-oil.

Variable	Factor	Level		
		+	0	-
Temperature	X_1	305°C	335°C	365°C
Reaction time	X_2	0.5h	2.25h	4h
Bio-oil/Red Mud ratio	X_3/X_2^a	10g/10g	20g/10g	30g/10g

^a In the full factorial design matrix//in the central design composite matrix.

Table 2: Full factorial design matrix for three factors in eleven observations/experiments for the neutralization of Red Mud with pyrolysis bio-oil.

run	Factor Level			Objective
	X_1	X_2	X_3	
1	-	-	-	DOE
2	+	-	-	DOE
3	-	+	-	DOE
4	+	+	-	DOE
5	-	-	+	DOE
6	+	-	+	DOE
7	-	+	+	DOE
8	+	+	+	DOE
9	0	0	0	Reprod ^a
10	0	0	0	Reprod ^a
11	0	0	0	Reprod ^a

^a Three identical experiments as the reproducibility set of the centre point.

Table 3: Central composite design matrix for two factors in thirteen observations/experiments for the neutralization of Red Mud with pyrolysis bio-oil.

run	Factor Level	
	X_1	X_2
1	-	-
2	+	-
3	-	+
4	+	+
5	-	0
6	+	0
7	0	+
8	0	-
9	0	0
10	0	0
11	0	0
12	0	0
13	0	0

Table 4: Sodium content, mass and pH of the aqueous phase and mass susceptibility, carbon percentage and pH of the solid phase determined using a full factorial matrix design.

run	Solid Phase			Liquid Phase		
	pH	%C (wt%)	$\chi_{if} \times 10^{-5}$ (m ³ /kg)	pH	m (g)	[Na] (g/L)
1	7.63	20.21	1.31	6.94	1.154	26
2	9.03	20.82	4.58	9.04	0.511	17
3	9.03	19.66	1.68	8.95	1.063	12
4	9.36	19.07	8.62	8.95	0.167	24
5	4.96	38.86	1.55	4.52	5.240	13
6	7.25	37.33	3.94	5.10	1.813	8.2
7	5.48	38.92	1.85	4.74	7.564	10
8	6.16	40.55	4.04	4.90	6.396	9.8
9	6.76	33.76	5.08	5.08	3.133	10
10	7.14	32.63	4.85	5.21	2.705	13
11	7.12	30.85	4.76	5.29	1.905	12

Table 5: Linear regression results and significant effects of regression coefficient from full factorial design.

Source	pH _{sol}		%C _{sol}		χ_{lf}	
	β	p^a	β	p^a	$\beta \times 10^{-5}$	p^a
X_0	7.36	<10 ⁻³	29.43	<10 ⁻³	3.45	<10 ⁻³
X_1	0.58	0.013	0.01	0.976	1.85	0.004
X_2	0.14	0.397	0.12	0.807	0.60	0.164
X_3	-1.40	<10 ⁻³	9.49	<10 ⁻³	-0.60	0.164
X_1X_2	-0.33	0.085	-	-	-	-
X_2X_3	-	-	-	-	-	-
X_1X_3	-	-	-	-	-0.70	0.115
<i>curvature</i>	-0.36	0.289	2.99	0.017	1.45	0.095
R^2	0.953		0.985		0.885	
R_{adj}^2	0.906		0.975		0.769	

Source	pH _{aq}		m _{aq}		[Na] _{aq}	
	β	p^a	β	p^a	β	p^a
X_0	6.64	<10 ⁻³	2.99	<10 ⁻³	15.00	<10 ⁻³
X_1	0.36	0.081	-0.77	0.043	-0.25	0.832
X_2	0.24	0.196	0.81	0.036	-1.05	0.392
X_3	-1.83	<10 ⁻³	2.27	0.001	-4.75	0.008
X_1X_2	-0.32	0.110	-	-	3.20	0.036
X_2X_3	-	-	0.92	0.023	-	-
X_1X_3	-	-	-	-	-	-
<i>curvature</i>	-1.45	0.006	-0.41	0.489	-3.33	0.181
$R^{2;b}$	0.970		0.947		0.855	
$R_{adj}^{2;c}$	0.939		0.895		0.710	

^a p-value. ^b R^2 = Sums of squares regression / Sums of squares total. ^c $R_{adj}^2 = 1 - (1 - R^2) \times (n-1) / (n-p)$, n number of run, p number of coefficient.

Table 6: Optimum levels determined for the significant variables using the full factorial design.

Variable	Level					
	Solid Phase			Liquid Phase		
	pH	%C	χ_{lf}	pH	m	[Na]
Target	7	max	max	7	min	Min
Temperature (°C)	305	-	365	-	365	305/335/365
Reaction time (h)	-	-	-	-	0.5	4/2.25/0.5
Bio-oil/Red Mud ratio	1	3	-	2	1	3

Table 7: Sodium content, mass and pH of the aqueous phase and mass susceptibility, carbon percentage and pH of the solid phase determined using a central composite matrix design with reaction held constant at 30 min.

run	Solid Phase			Liquid Phase		
	pH	%C (wt%)	$\chi_m \times 10^{-5}$ (m ³ /kg)	pH	M (g)	[Na] (g/L)
1 ^a	7.63	20.21	1.31	6.94	1.154	26
2 ^b	9.03	20.82	4.58	9.04	0.511	17
3 ^c	4.96	38.86	1.55	4.52	5.240	13
4 ^d	7.25	37.33	3.94	5.10	1.813	8.2
5	5.50	32.53	2.06	4.93	1.472	16
6	6.55	32.30	5.74	5.45	1.618	15
7	9.34	18.69	3.61	9.79	0.448	16
8	5.42	40.13	1.75	4.67	4.336	12
9	5.75	32.99	3.89	4.99	1.9486	16
10	6.12	30.74	3.88	5.01	1.579	14
11	6.34	32.21	4.21	5.18	1.74	15
12	5.75	33.28	3.14	5.03	1.6169	16
13	6.00	32.83	5.12	5.25	1.8238	14

Transcribed from Table 4: ^a run 1 ^b run 2 ^c run 5 ^d run 6.

Table 8: Experimental model fitted to the response of the 13 runs of Table 7 with uncoded factors.

Response	Experimental model	Eq	R^2	R_{adj}^2
pH _{aq}	$Y_1 = -42.27 + 0.3037 T - 4.430 B - 3.889 \times 10^{-4} T^2 + 1.690 B^2 - 1.267 \times 10^{-2} TB$	(4)	0.938	0.895
pH _{sol}	$Y_2 = 2.477 + 5.719 \times 10^{-2} T - 9.054 B - 6.820 \times 10^{-5} T^2 + 1.293 B^2 + 7.417 \times 10^{-3} TB$	(5)	0.935	0.889
%C _{sol}	$Y_3 = -14.46 + 6.509 \times 10^{-2} T + 27.62 B - 5.345 \times 10^{-5} T^2 - 3.053 B^2 - 1.783 \times 10^{-2} TB$	(6)	0.984	0.973
[Na] _{aq}	$Y_4 = 229.0 - 1.081 T - 15.20 B + 1.387 \times 10^{-5} T^2 - 0.2517 B^2 + 3.500 \times 10^{-2} TB$	(7)	0.825	0.700
m _{aq}	$Y_5 = -32.51 + 0.1768 T + 6.750 B - 2.271 \times 10^{-4} T^2 + 0.6427 B^2 - 2.320 \times 10^{-2} TB$	(8)	0.903	0.833
χ_{lf}	$Y_6 = -2.202 \times 10^{-4} + 6.425 \times 10^{-7} T + 6.948 \times 10^{-5} B + 3.448 \times 10^{-11} T^2 - 1.217 \times 10^{-5} B^2 - 7.333 \times 10^{-8} TB$	(9)	0.861	0.762

T = temperature (in °C). B = BO/RM ratio (in g/g).

Table 9: Analysis of variance for the neutralization of Red Mud.

Source	DF ^a	pH _{sol}		%C _{sol}		χ_{lf}	
		F ^b	p ^c	F ^b	p ^c	F ^b	p ^c
<i>Model</i>	5	20.13	0.001	87.13	<10 ⁻³	8.69	0.007
<i>X</i> ₁	1	18.09	0.004	0.17	0.693	31.03	0.001
<i>X</i> ₂	1	56.39	<10 ⁻³	411.1	<10 ⁻³	1.82	0.220
<i>X</i> ₁ ²	1	0.05	0.829	<10 ⁻²	0.946	<10 ⁻²	0.994
<i>X</i> ₂ ²	1	22.32	0.002	19.82	0.003	8.73	0.021
<i>X</i> ₁ <i>X</i> ₂	1	0.96	0.361	0.88	0.379	0.41	0.541
<i>LOF</i> ^d	3	6.25	0.054	1.62	0.318	0.80	0.556

Source	DF ^a	pH _{aq}		m _{aq}		[Na] _{aq}	
		F ^b	p ^c	F ^b	p ^a	F ^b	p ^c
<i>Model</i>	5	21.34	<10 ⁻³	13.00	0.002	6.61	0.014
<i>X</i> ₁	1	5.62	0.050	8.35	0.023	7.71	0.027
<i>X</i> ₂	1	72.31	<10 ⁻³	46.64	<10 ⁻³	23.44	0.002
<i>X</i> ₁ ²	1	1.11	0.326	0.38	0.559	0.91	0.372
<i>X</i> ₂ ²	1	25.97	0.001	3.71	0.095	0.04	0.853
<i>X</i> ₁ <i>X</i> ₂	1	1.90	0.210	6.31	0.040	0.93	0.367
<i>LOF</i> ^d	3	51.48	0.001	29.99	0.003	9.71	0.026

^a Degrees of freedom. ^b F-value = Mean squares regression / Mean squares residual error. ^c p-value. ^d Lack of fit with F = Mean squares regression / Mean squares pure error.

Table 10: Sodium content, mass and pH of the aqueous phase and mass susceptibility, carbon percentage and pH of the solid phase in neutralization of Red Mud with pyrolysis bio-oil at BO/RM = 1.53 and T = 349°C.

Exp	Solid Phase			Liquid Phase		
	pH	%C (wt%)	χ_{lf} (10 ⁻⁵ m ³ /kg)	pH	m (g)	[Na] (g/L)
14	7.89	25.03	5.25	6.09	1.057	16
15	7.80	25.90	5.81	5.52	0.890	13
16	7.66	25.76	5.72	6.39	2.345	18
17	7.62	26.54	5.29	6.22	2.341	18
Aver ^a	7.74	25.81	5.52	6.06	1.66	16.3
SD ^b	0.13	0.62	0.29	0.38	0.79	2.4
Fit ^c	7.26	27.33	4.69	6.74	0.961	15.6
95% PI ^d	6.09 - 8.44	24.39 - 30.28	2.94 - 6.46	5.32 - 8.17	0 - 2.39	10.0 - 21.3
18 ^e	7.51	26.69	4.62	5.59	7.384/2	19
19 ^f	7.68	27.27	3.89	5.80	10.907/3	18

^a Average of run 14 to 17. ^b Standard Deviation. ^c Fitted values from equations 4-9 in Table 8. ^d Prediction interval. ^e Scale up by factor 2. ^f Scale up by factor 3.